J|A|C|S
ARTICLES
Published on Web 10/01/2002

Pulsed Electron−Electron Double Resonance on Multinuclear Metal Clusters: Assignment of Spin Projection Factors Based on the Dipolar Interaction

Celine Elsässer,[†] Marc Brecht,[‡,§] and Robert Bittl*,[†]

Contribution from the Institut für Experimentalphysik, Freie Universität Berlin, Arnimallee 14, 14195 Berlin, Germany, and Max-Volmer-Laboratorium, Technische Universität Berlin, Strasse des 17. Juni 135, 10623 Berlin, Germany

Received June 18, 2002

Abstract: The interaction between two paramagnetic metal centers, a $[3Fe-4S]^+$ cluster and a [NiFe] center, is investigated in the hydrogenase from *Desulfovibrio vulgaris* Miyazaki F by pulsed ELDOR (electron−electron double resonance). The distance between the metal centers is known from X-ray crystallography. The experimental dipolar spin−spin interaction deviates from the value expected for two point-dipoles located at the centers of the metal clusters. An extended spin-coupling model accounting for the spin coupling in the $[3Fe-4S]^+$ cluster yields the observed interaction under the assumption of a particular magnetic coupling scheme for the three Fe ions. These results demonstrate that pulsed ELDOR can be used to gain insight into the inner structure of a multinuclear metal cluster.

1. Introduction

The [NiFe] hydrogenase from *Desulfovibrio* (*D.*) *vulgaris* Miyazaki F enzymatically catalyses the heterolytical cleavage of hydrogen molecules: $H_2 \rightleftharpoons H^+ + H^-$.

The structures of this "standard" hydrogenase in the oxidized as well as in the reduced state are known from X-ray crystallography at 1.4 and 1.8 Å resolutions, respectively.[1,2] This hydrogenase is similar to that from *D. gigas* for which the structure has also been solved.[3] The cleavage of hydrogen takes place at the [NiFe] center in the large subunit of the protein. The electrons are subsequently transferred to the surface of the protein by an electron-transfer chain which involves one [3Fe−4S] cluster and two [4Fe−4S] clusters. The [4Fe−4S] cluster close to the [NiFe] center is called the "proximal", the one close to the protein surface, the "distal" cluster. The [3Fe−4S] cluster is located between the two [4Fe−4S] clusters.

In the oxidized state, the hydrogenase contains two paramagnetic species, the [NiFe] center and the $[3Fe-4S]^+$ cluster (Figure 1), whereas both $[4Fe-4S]^{2+}$ clusters are diamagnetic in their ground states. The $S = {}^1/_2$ signal of the [NiFe] center consists of two different paramagnetic states called Ni-A and Ni-B (for Ni-A: $g_1 = 2.317$, $g_2 = 2.229$, $g_3 = 2.014$; for Ni-B: $g_1 = 2.333$, $g_2 = 2.163$, $g_3 = 2.010$). The as-isolated hydrogenase from *D. vulgaris* Miyazaki F contains about 30% Ni-A and 70% Ni-B.

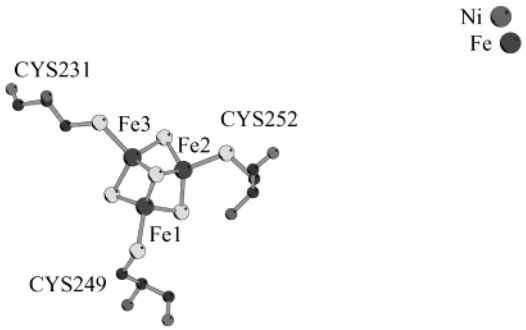

Figure 1. Cofactors in the hydrogenase from *D. vulgaris* Miyazaki F. The [NiFe] center and the $[3Fe-4S]^+$ cluster with ligating cysteines are shown. Numbering of the Fe ions is equivalent to the X-ray structure (PDB {http://www.rcsb.org} entry 1H2A). Distances of the Fe ions to Ni: r(Fe1) = 2.229 nm, r(Fe2) = 2.012 nm, r(Fe3) = 2.172 nm.

The electron spin density distribution around the [NiFe] center is well-known from ^{1}H ENDOR,[4] ^{61}Ni EPR,[5] ^{33}S EPR,[6] and ^{57}Fe ENDOR[7] which revealed the hyperfine coupling of the respective nuclei. The spin densities have subsequently been calculated by DFT methods, and it was shown that the spin density of the [NiFe] center is mainly located on the Ni ion.[8] EPR analysis of hydrogenase single crystals yielded the orientation of the g-tensor of the [NiFe] center with respect to the molecular structure.[9,10]

* Corresponding author. Fax: ++49-30-838 56046. E-mail: Robert.Bittl@Physik.FU-Berlin.de.
[†] Freie Universität Berlin.
[‡] Technische Universität Berlin.
[§] Present address: Institut für Experimentalphysik, Freie Universität Berlin, Arnimallee 14, 14195 Berlin, Germany.

(1) Higuchi, Y.; Yagi, T.; Yasuoka, N. *Structure* **1997**, *5*, 1671−1680.
(2) Hichugi, Y.; Ogata, H.; Miki, K.; Yasuoka, N.; Yagi, T. *Struct. Fold. Des.* **1999**, *7*, 549−556.
(3) Volbeda, A.; Charon, M.-V.; Piras, C.; Hatchikian, E. C.; Frey, M.; Fontecilla-Camps, J. C. *Nature* **1995**, *373*, 580−587.
(4) Gessner, C.; Stein, M.; Albracht, S. P. J.; Lubitz, W. *J. Biol. Inorg. Chem.* **1999**, *4*, 379−389.
(5) Albracht, S. P. J.; Graf, E. G.; Thauer, R. K. *FEBS Lett.* **1982**, *140*, 211.
(6) Albracht, S. P. J.; Kröger, A.; der Zwaan, J. W. V.; Unden, G.; Böcher, R.; Mell, H.; Fontijn, R. D. *Biochim. Biophys. Acta* **1986**, *874*, 116.
(7) Huyett, J. E.; Carepo, M.; Pamplona, A.; Franco, R.; Moura, I.; Moura, J. J. G.; Hoffman, B. M. *J. Am. Chem. Soc.* **1997**, *119*, 9291−9292.
(8) Stein, M.; Lubitz, W. *Phys. Chem. Chem. Phys.* **2001**, *3*, 2668−2675.

10.1021/ja027348+ CCC: $22.00

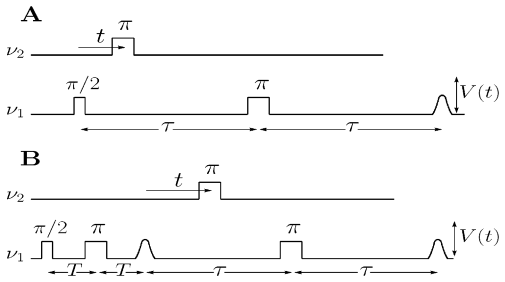

Figure 2. ELDOR pulse sequences. ν_1 and ν_2 are the microwave frequencies. (A) three-pulse ELDOR and (B) Four-pulse ELDOR. The time t is incremented during the experiment.

The $[3Fe-4S]^+$ cluster in the hydrogenase from *D. gigas* has been characterized by EPR spectroscopy.[11] The cluster consists of three formally Fe(III) ions with spins $S = {}^5/_2$ which are antiferromagnetically coupled and give rise to an EPR signal of a $S = {}^1/_2$ ground state[12] with $g_1 = 2.032$, $g_2 = 2.024$, and $g_3 = 2.016$.[11] A recent study of the $[3Fe-4S]^+$ cluster in *D. vulgaris* Miyazaki F has shown that the electronic properties of the clusters are similar to that in *D. gigas* and the full rhombic g-tensor ($g_1 = 2.0257$, $g_2 = 2.0174$, $g_3 = 2.0114$) has been resolved by high-field/high-frequency EPR.[13] ENDOR experiments on protons in the vicinity of the $[3Fe-4S]^+$ cluster revealed that also the protein environments of the $[3Fe-4S]^+$ clusters are similar in the two hydrogenases.[13,14]

Mössbauer spectroscopy was used to elucidate the electronic structure within the $[3Fe-4S]^+$ cluster of the hydrogenase from *D. gigas*. The spin distribution of the $[3Fe-4S]^+$ cluster was analyzed by measuring the hyperfine coupling of the Fe ions, and spin projection factors K_i of $+2.28$, -0.28, and -1.00 for the three Fe ions were calculated.[12,15] In the hydrogenase, the assignment of the spin projection factors to the individual Fe ions is not known from Mössbauer spectroscopy.

Pulsed electron−electron double resonance (ELDOR) is a two-frequency EPR experiment used to determine distances between two spin centers. This method is also referred to as double electron−electron resonance (DEER). A detailed discussion of this method is given for example in refs 16 and 17. In the pulsed ELDOR experiment, the electron−electron dipolar coupling between two spins is measured. This is determined by the distance between and the relative orientation of the spins. The geometrical arrangement can be resolved for spins with a separation in the range of about 1.5−8 nm.[17] A constant time two-pulse echo with fixed interpulse delay performed with a microwave frequency ν_{det} probes one paramagnetic center (the pulse sequence is shown in Figure 2). Within the evolution period, an inversion pulse with a microwave frequency ν_{inv} is applied on the second paramagnetic center and its position within the echo sequence is changed in time. Because of the dipolar coupling between the two spin systems, the amplitude of the two-pulse echo is modulated.

From the frequency of this modulation, the distance between the two spins usually is derived using the point-dipole approximation

$$\nu_d = \frac{g_{det} g_{inv} \mu_B^2 \mu_0}{4\pi h} \frac{3\cos^2\vartheta - 1}{r^3} \qquad (1)$$

where g_{det} and g_{inv} are the effective g-values selected by the respective frequencies ν_{det} and ν_{inv}, $r = |\vec{r}|$ is the length of the vector $\vec{r}$ connecting the two spins, and ϑ is the angle between the connecting vector $\vec{r}$ and the static external magnetic field $\vec{B}$.

Pulsed ELDOR experiments have been primarily performed on systems with two organic radicals, for example, two spin labels separated by anthracene,[18] polystyrene,[19] or a polypeptide.[20] Examples of pulsed ELDOR experiments involving metal ions are measurements on photosystem II involving the Mn_4 cluster and the tyrosine $Y_D^\bullet$ radical[21,22] and on sulfite oxidase involving an Fe(III) and an Mo(V) ion.[23]

In this work, we present pulsed ELDOR experiments on the [NiFe] center and the $[3Fe-4S]^+$ cluster in the hydrogenase from *D. vulgaris* Miyazaki F. The ELDOR modulations are analyzed with respect to the X-ray structure and results from Mössbauer spectroscopy. We show that the dipolar interaction between two paramagnetic centers depends on the inner structure of the $[3Fe-4S]^+$ cluster. Calculating the distance between the metal center with the point-dipole approximation regarding the $[3Fe-4S]^+$ cluster as a localized $S = {}^1/_2$ spin yields a distance which deviates from that known from the X-ray structure. Therefore, the analysis of the pulsed ELDOR data allows insight into the inner structure of multinuclear metal centers.

2. Theoretical Background

In a multinuclear paramagnetic center, the magnetic moment is delocalized over the ions of the cluster. Hence, describing the dipolar coupling between such a metal cluster and a second spin system within the point-dipole approximation (eq 1) in general yields inaccurate results.[24] Consequently, the magnetic interactions between all ions of a metal center and the second spin have to be explicitly considered.[24] This approach has been successfully applied to calculations of hyperfine tensors in ENDOR experiments on multinuclear metal centers.[25−27] We herein adapt the spin-coupling model for the interpretation of pulsed ELDOR experiments.

(9) Gessner, C.; Trofanchuk, O.; Kawagoe, K.; Higuchi, Y.; Yasuoka, N.; Lubitz, W. *Chem. Phys. Lett.* **1996**, *256*, 518−524.
(10) Trofanchuk, O.; Stein, M.; Gessner, C.; Lendzian, F.; Higuchi, Y.; Lubitz, W. *J. Biol. Inorg. Chem.* **2000**, *5*, 36−44.
(11) Fan, C.; Houseman, A. L. P.; Doan, P.; Hoffman, B. M. *J. Phys. Chem.* **1993**, *97*, 3017−3021.
(12) Kent, T. A.; Huynh, B. H.; Münck, E. *Proc. Natl. Acad. Sci. U.S.A.* **1980**, *77*, 6574−6576.
(13) Brecht, M. Doctoral Thesis, Technische Universität Berlin, 2001.
(14) Doan, P. E.; Fan, C.; Hoffman, B. M. *J. Am. Chem. Soc.* **1994**, *116*, 1033−1041.
(15) Mouesca, J. M.; Noodleman, L.; Case, D. A.; Lamotte, B. *Inorg. Chem.* **1995**, *34*, 4347−4359.
(16) Milov, A. D.; Salikhov, K. M.; Shchirov, M. D. *Fiz. Tverd. Tela. (S.−Peterburg)* **1981**, *23*, 975; *Sov. Phys. Solid State* **1981**, *23*, 565.
(17) Jeschke, G.; Pannier, M.; Spiess, H. W. *Biological Magnetic Resonance 19;* Berliner, L. J., Eaton, S. S., Eaton, G. R., Eds.; Kluwer Academic/Plenum Publishers: New York, 2000; pp 493−512.
(18) Larsen, R. G.; Singel, D. J. *J. Chem. Phys.* **1993**, *98*, 5134−5146.
(19) Pannier, M.; Schädler, V.; Schöps, M.; Wiesner, U.; Jeschke, G.; Spiess, H. W. *Macromolecules* **2000**, *33*, 7812−7818.
(20) Milov, A. D.; Maryasov, A. G.; Tsvetkov, Y. D.; Raap, J. *Chem. Phys. Lett.* **1999**, *303*, 135−143.
(21) Hara, H.; Kawamori, A.; Astashkin, A. V.; Ono, T. *Biochim. Biophys. Acta* **1996**, *1276*, 140−146.
(22) Mino, H.; Kawamori, A.; Ono, T. *Biochemistry* **2000**, *39*, 11034−11040.
(23) Codd, R.; Astashkin, A. V.; Pacheco, A.; Raitsimring, A. M.; Enemark, J. H. *J. Biol. Inorg. Chem.* **2002**, *7*, 338−350.
(24) Bertrand, P.; More, C.; Guigliarelli, B.; Fournel, A.; Bennett, B.; Howes, B. *J. Am. Chem. Soc.* **1994**, *116*, 3078−3086.
(25) Fiege, R.; Zweygart, W.; Bittl, R.; Adir, N.; Renger, G.; Lubitz, W. *Photosythesis Research* **1996**, *48*, 227−237.
(26) Randall, D. W.; Gelasco, A.; Caudle, M. T.; Pecoraro, V. L.; Britt, R. D. *J. Am. Chem. Soc.* **1997**, *119*, 4481−4491.
(27) Cannes, C.; Ebelshauser, M.; Gay, E.; Shergill, J. K.; Cammack, R.; Kappl, R.; Hüttermann, J. *J. Biol. Inorg. Chem.* **2000**, *5*, 514−526.

The energy of the spin system in an external magnetic field $\vec{B}$ is described by a Hamiltonian

$$\hat{H} = \hat{H}_Z + \hat{H}_{int} + \hat{H}_{ex} + \hat{H}_{dip} \quad (2)$$

which accounts for the Zeeman interactions $\hat{H}_Z$, the intracluster spin−spin coupling (exchange and dipole interaction) $\hat{H}_{int}$ within the $[3Fe-4S]^+$ cluster, the exchange interaction $\hat{H}_{ex}$, and dipolar interaction $\hat{H}_{dip}$ of the [NiFe] center with the $[3Fe-4S]^+$ cluster. The dipolar coupling can be described by

$$\hat{H}_{dip} = \frac{\mu_0}{4\pi}\sum_{i=1}^{3}\frac{1}{r_{i,4}^3}(\vec{\mu}_i\vec{\mu}_4 - 3(\vec{\mu}\vec{n}_{i,4})(\vec{\mu}_4 n_{i,4})) \quad (3)$$

with $\vec{\mu}_i = -\mu_B g_i \vec{S}_i$; $\vec{n}_{i,4} = \vec{r}_{i,4}/r_{i,4}$; $i,j = 1, 2, 3$ denoting the three $S = {}^5/_2$ spins of the $[3Fe-4S]^+$ cluster; and $i, j = 4$ denoting the $S = {}^1/_2$ of the [NiFe] center. The exchange interaction between the proximal [4Fe−4S] cluster and the [NiFe] center, which are separated by about 12 Å, was determined as $J = 4 \times 10^{-3}$ cm^{-1}.[28] Because of the exponential distance dependence of the exchange interaction,[29] the exchange interaction between the $[3Fe-4S]^+$ cluster and the [NiFe] center is expected to be in the order of 6 magnitudes smaller, that is, less than 10^{-4} MHz, and therefore neglected in the following analysis.

The Hamiltonian (eq 2) is dominated by the intracluster spin−spin coupling $\hat{H}_{int}$ of the $[3Fe-4S]^+$ cluster. Therefore, the three spins $S_i = {}^5/_2$ of the Fe ions couple to an effective spin $\vec{S}_{FeS} = \vec{S}_1 + \vec{S}_2 + \vec{S}_3$ with a ground state $S^0_{FeS} = {}^1/_2$ which is well separated from the first excited state.[30] The $[3Fe-4S]^+$ cluster can be described within the spin-coupling model in which the individual spins are substituted according to the Wigner−Eckart theorem

$$\vec{S}_i = K_i \vec{S}_{FeS} \quad (4)$$

where K_i are the spin projection factors of the individual $[3Fe-4S]^+$ cluster ions.[12]

Using eq 4, the Zeeman interaction $\hat{H}_Z$ can be replaced analytically within the $S^0_{FeS} = {}^1/_2$ multiplet and yields

$$\hat{H}_Z = \mu_B \vec{B} g_{Ni} \vec{S}_{Ni} + \mu_B \vec{B} g_{FeS} \vec{S}_{FeS} \quad (5)$$

with $g_{FeS} = \sum_i K_i g_i$. In contrast, it is impossible to replace the dipolar coupling $\hat{H}_{int}$ between a metal cluster and a second spin by a Hamiltonian which solely depends on the interaction of two point-dipoles. Each magnetic moment, $\vec{\mu}_i$, of the coupled spin system has to be considered individually using the spin projection factors introduced in eq 4.

The spin projection factors K_i of the three iron ions were determined for the $[3Fe-4S]^+$ cluster by Mössbauer and theoretical studies,[12,15] but Mössbauer spectroscopy is insensitive to the location of the iron ions. Assignment to which iron ion the individual spin projection factors correspond is in principle possible with paramagnetic NMR.[31] Analyzing the hyperfine interaction of β-CH_2 protons of ligating cysteines yields this assignment. No such assignment has been performed for any of the iron−sulfur clusters in hydrogenase yet.

In the following, we show that the dipolar coupling measured in pulsed ELDOR experiments can be used for this assignment. Using eq 4, $\hat{H}_{dip}$ can be expressed as

$$\hat{H}_{dip} = \frac{\mu_0 \mu_B^2}{4\pi}\sum_{i=1}^{3}\frac{g_i g_{Ni}}{r_{i,Ni}^3}K_i(\vec{S}_{FeS}\vec{S}_{Ni} - 3(\vec{S}_{FeS}\vec{n}_{i,Ni})(\vec{S}_{Ni}\vec{n}_{i,Ni})) \quad (6)$$

with i denoting the three iron ions of the $[3Fe-4S]^+$ cluster and FeS and Ni denoting the $[3Fe-4S]^+$ cluster and the [NiFe] center, respectively. The g-tensor of the $[3Fe-4S]^+$ cluster shows little anisotropy. Therefore, we assume that the g-tensors of the individual iron ions have small anisotropies and are equal, $g_{FeS} = g_i$. Equation 6 shows that the dipolar interaction is the sum of the dipolar tensors between the Ni ion and the individual ions of the coupled cluster ($[3Fe-4S]^+$) weighted by the projection factors K_i. The individual dipolar tensors are, in general, diagonal in different principal axis systems due to their dependence on $\vec{r}_i$. If the distances r_i between the iron ions are small compared to the distance between the two paramagnetic centers, this can be neglected. Consequently, the dipolar coupling can be reduced to the expression

$$\nu_d = \frac{g_{Ni} g_{FeS} \mu_B^2 \mu_0}{4\pi h}\sum_{i=1}^{3}K_i\frac{3\cos^2\vartheta_i - 1}{r_{i,Ni}^3} \quad (7)$$

where ϑ_i values are the angles between the magnetic field axis $\vec{B}$ and the vectors $\vec{r}_{i,Ni}$. The dipolar frequency depends on the distances of the individual Fe ions from the [NiFe] center weighted by the spin projection factors. This equation can be used to evaluate the dipolar interaction of a metal cluster which is described by the spin-coupling model and a second spin. If the positions of the metal ions are known, for example, from X-ray crystallography, the dipolar interaction solely depends on the spin coupling in the metal cluster. Pulsed ELDOR therefore is a method to assign the spin projection factors to the individual ions in a multinuclear metal cluster.

Pulsed ELDOR experiments involving one or two metal centers differ in two main respects from experiments on organic radical pairs. In the following, differences arising from relaxation behavior and distinct g-anisotropies which often are found in metals are discussed.

The pulsed ELDOR method measuring the dipolar interaction between two spins always competes with the relaxation by dipolar spin−spin interaction which is enhanced in transition metal centers. In metal clusters, spins of the individual ions couple to a total spin and the intracluster spin−spin interaction is a fast relaxation pathway. At 5 K, the $[3Fe-4S]^+$ cluster has a phase memory time T_M of approximately 360 ns and the [NiFe] center of 800 ns. This diminishes the time available for acquiring pulsed ELDOR data significantly compared to those of experiments on organic radicals and results in reduced frequency resolution.

With the microwave pulses, molecules in certain orientations with respect to the magnetic field $\vec{B}$ are selectively excited. In a two-spin system, which can be completely excited by the pulses, the ELDOR experiment results in the full Pake pattern of the dipolar coupling between the spins from which the

(28) Dole, F.; Medina, M.; More, C.; Cammack, R.; Bertrand, P.; Guigliarelli, B. *Biochemistry* **1996**, *35*, 16399−16406.
(29) Moser, C. C.; Keske, J. M.; Warnke, K.; Farid, R. S.; Dutton, P. L. *Nature* **1992**, *355*, 796−802.
(30) Telser, J.; Lee, H.-I.; Hoffman, B. M. *J. Biol. Inorg. Chem.* **2000**, *5*, 369−380.
(31) Macedo, A. L.; Moura, I.; Moura, J. J. G.; LeGall, J.; Huynh, B. H. *Inorg. Chem.* **1993**, *32*, 1101−1105.

principal values can be obtained directly. In the hydrogenase, the oxidized [NiFe] center shows a g-anisotropy over $\Delta g = 0.3$, whereas the excitation width of a (32 ns) π-pulse in X-band is about $\Delta g \approx 0.003$ (at $g \approx 2$). Mainly, because of g-anisotropy of the [NiFe] center, it is impossible to excite the complete EPR spectrum. This leads to deviations of the frequency spectrum from a full Pake pattern, since, in the spectrum, lines appear only where both spin systems are excited. The pulsed ELDOR spectrum depends on the angles between all selected orientations and the dipolar axis. The orientational selective excitation yields a single crystal-like selection of individual lines. This effect can sometimes be seen even in systems with two organic radicals, for example, two nitroxide spin labels.[18−20]

3. Material and Methods

3.1. Simulation. For the simulation of pulsed ELDOR spectra, a program which calculates the dipolar interaction between multinuclear metal centers has been written. The simulation routine accounts for the effects of spin coupling and orientation selection. The pulsed ELDOR spectrum is calculated by the uniform sampling of B-field orientations within the metal center which is used for detection. The program assumes a well-defined orientation between the g-tensors of both spins described by three Euler angles. Also, the orientation of the dipolar axis is assumed to be well-defined with respect to the g-tensors and described by two Euler angles within the g-tensor system of the detected spin. In the present case, the three Euler angles between the g-tensors have been evaluated from single-crystal studies on the individual spin centers[10,13] and the two Euler angles for the dipolar coupling from the X-ray structure.[1] Only that fraction of the powder sample is considered for which the g-values of both spins are within the excitation bandwidth. The excitation bandwidth is convoluted with a line width function to account for g-strain[32] and hyperfine interactions.

The dipolar interaction (eq 7) for the selected orientations is calculated according to the spin projection factors of the Fe_i ions in the cluster, the distances between the Fe_i ions and the Ni, and the angle between the Fe_i−Ni connection vectors $\vec{r}_{i,Ni}$ and the magnetic field $\vec{B}$. From this a weighted frequency histogram is constructed and convoluted with a Gaussian line-shape to account for inhomogeneous line broadening.

3.2. Experiments. The [NiFe] hydrogenase from *D. vulgaris* Miyazaki F has been prepared as described previously.[33] The protein solution was buffered with 25 mM trisHCl (pH 7.4) with 50 mM NaCl and 0.05% NaN_3.

The pulsed ELDOR measurements were performed on a Bruker ESP 380E X-band FT spectrometer equipped with an ER 4118-MD5-W1-EN dielectric ring resonator and an Oxford CF 935 helium flow cryostat controlled by an Oxford ITC4. For the second frequency, the cw microwave output of a Bruker ER 042 MRH E bridge with frequency stabilizer was connected to one of the pulse forming units of the ESP 380-1010 bridge.

All experiments have been performed at a temperature of 5 K. The microwave π-pulses of both frequencies were adjusted to 32 ns, the $\pi/2$-pulse, to 16 ns. For ELDOR experiments, the following pulse sequences, also depicted in Figure 2, have been used. (i) Three-pulse ELDOR: $(\pi/2)_x - t - \pi - (\tau - t) - \pi_x - \tau -$ detection. (ii) For dead-time free experiments, a four-pulse sequence (four-pulse DEER) was introduced.[34] Because of a weak signal intensity, we used an asymmetric version of the four-pulse ELDOR, where more time can be used for acquiring ELDOR data: $(\pi/2)_x - T - \pi_x - t - \pi - (\tau + T - t) - \pi_x - \tau -$ detection. Accumulated time-domain data were fitted with a monoexponential decay function which was subsequently subtracted. The frequency domain spectra were obtained by Fourier transformation after zero-filling and multiplication with a Hamming window function.

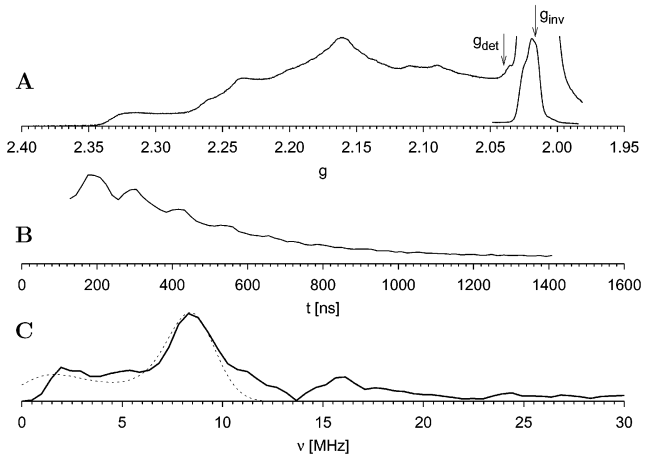

Figure 3. (A) Two-pulse field-swept echo EPR spectrum of hydrogenase ($\nu_{mw} = 9.7057$ GHz). The spectrum of the $[3Fe-4S]^+$ cluster is scaled down (by about fifty) to render the [NiFe] spectrum visible. (B) Three-pulse ELDOR time trace recorded at B = 3400 G with a detection frequency $\nu_{det} = 9.7077$ GHz ($g_{det} = 2.040$) and an inversion frequency $\nu_{inv} = 9.5983$ GHz ($g_{inv} = 2.017$); the g-values are indicated in the 2P-EPR spectrum. (C) ELDOR frequency spectrum and simulation (dotted line) assuming 30% Ni-A and 70% Ni-B.

4. Results and Discussion

The two-pulse EPR spectrum of the hydrogenase from *D. vulgaris* Miyazaki F is shown in Figure 3A. The signal on the high-field side is associated with the $[3Fe-4S]^+$ cluster and scaled down compared to the broad signal on the low field side which is associated with the [NiFe] center. To perform pulsed ELDOR experiments, the two-pulse Hahn echo sequence with the frequency ν_{det} was applied on the [NiFe] center. The second frequency ν_{inv} was set to invert the spin of the $[3Fe-4S]^+$ cluster. Pulsed ELDOR experiments were performed on various field positions and frequency differences in a narrow experimentally accessible range (representative spectra are shown in Figures 3 and 4). In the 2P-EPR spectra (Figure 3A), a representative pair of g-values of the pulsed ELDOR experiment of Figure 3B are marked. Figure 3B shows the time dependence of the two-pulse echo amplitude at $B = 3400$ G, while the pump pulse with $\nu_{inv} = 9.5983$ GHz ($g_{inv} = 2.017$) is incremented in time between the two pulses of the detection frequency $\nu_{det} = 9.7077$ GHz ($g_{det} = 2.040$).

The main feature in the Fourier transformed pulsed ELDOR time trace (Figure 3C) at 8.5 MHz is assigned to the dipolar interaction between the NiFe center and the $[3Fe-4S]^+$ cluster, since it is absent in experiments where the two ELDOR frequencies were chosen to excite spins which are not within the spectral range of the $[3Fe-4S]^+$ cluster ground state, for example, at $B = 3250$ G with $\nu_{det} = 9.7077$ GHz ($g_{det} = 2.134$) and $\nu_{inv} = 9.6071$ GHz ($g_{inv} = 2.112$) (data not shown).

It is also possible to detect pulsed ELDOR modulations on the very intense $[3Fe-4S]^+$ signal at $B = 3380$ G with $\nu_{det} = 9.7029$ GHz ($g_{det} = 2.015$), when parts of the weak [NiFe] signal are inverted. A corresponding time trace with $\nu_{inv} = 9.8684$ GHz ($g_{inv} = 2.050$) is shown in Figure 4A. The modulation

(32) Hagen, W. R.; Hearshen, D. O.; Harding, L. J.; Dunham, W. R. *J. Magn. Reson.* **1985**, *61*, 220−232.
(33) Yagi, T.; Kimura, K.; Daidoji, H.; Sakai, F.; Tamura, S.; Inokuchi, H. *J. Biochem. (Tokyo)* **1976**, *79*, 661−671.
(34) Martin, R. E.; Pannier, M.; Diederich, F.; Gramlich, V.; Hubrich, M.; Spiess, H. W. *Angew. Chem.* **1998**, *110*, 2994−2998.

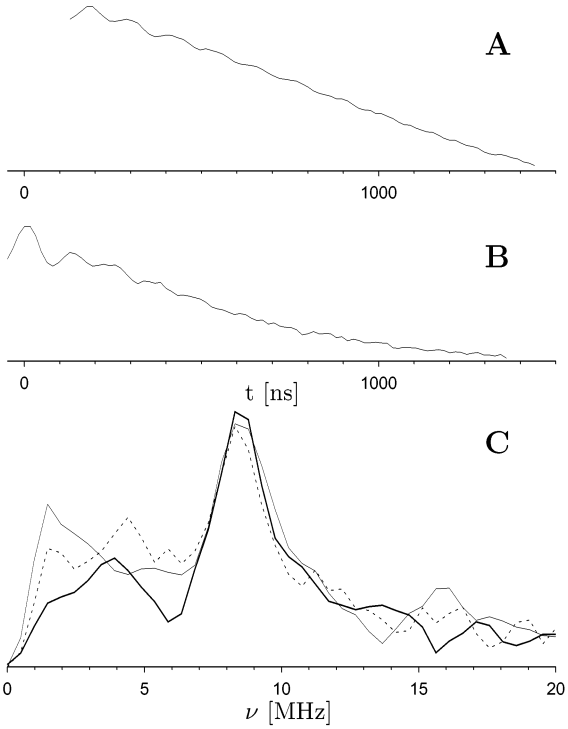

Figure 4. (A) Three-pulse ELDOR time trace, detection on the $[3Fe-4S]^+$ cluster at $B = 3440$ G with $\nu_{det} = 9.7029$ GHz ($g_{det} = 2.015$) and $\nu_{inv} = 9.8684$ GHz ($g_{inv} = 2.050$). (B) Asymmetric four-pulse ELDOR at $B = 3880$ G with $\nu_{det} = 9.7015$ GHz ($g_{det} = 2.051$) and $\nu_{inv} = 9.5390$ GHz ($g_{inv} = 2.016$). (C) Fourier transforms of time traces 3B (narrow line), 4A (dotted line), and 4B (thick line).

depth of the echo in this case is significantly smaller compared to that of the detection on the [NiFe] center. This is due to the fact that only a small part of the $[3Fe-4S]^+$ cluster echo intensity is effected by inversion of an orientation selected fraction of the [NiFe] spins. The ratio of the modulation depths in the two cases is consistent with the relative signal intensities involved in detection and inversion, respectively. The experiment yields a similar spectrum compared to that of the detection on the [NiFe] center (Figure 4C).

To achieve a dead-time free measurement, a four-pulse ELDOR sequence on a refocused echo[34] was performed (Figure 4B) at $B = 3440$ G, detecting with $\nu_{det} = 9.7015$ GHz ($g_{det} = 2.051$) and the inversion pulse set to excite spins of the $[3Fe-4S]^+$ cluster with $\nu_{inv} = 9.5390$ GHz ($g_{inv} = 2.016$). However, because of the prolonged delay between the initial $\pi/2$-pulse and the detection, the obtainable signal-to-noise ratio was significantly reduced.

Under the approximation that the two $S = {}^1/_2$ spins interact as point-dipoles (eq 1), a pulsed ELDOR experiment should yield a frequency of 6.6 MHz if the spin of the $[3Fe-4S]^+$ cluster is located on the Fe ion closest to the [NiFe] center (Fe2; for numbering of Fe ions, see Figure 1) and 4.8 MHz if the spin is located on the most remote Fe ion (Fe1). Figure 5A shows the calculated spectrum for two spins $S = {}^1/_2$ in a distance of 2.14 nm (average distance between Fe_i and Ni) with a peak at 5.2 MHz. These frequencies are well below the measured frequencies in the different experiments. Using the point-dipole approximation, the measured frequency 8.5 MHz in Figure 3 corresponds to a distance of 1.84 nm, which is 0.3 nm shorter than the average distance between the [NiFe] center and the $[3Fe-4S]^+$ cluster.

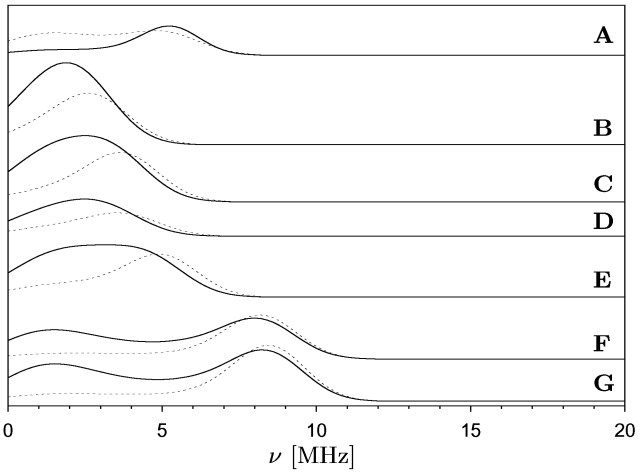

Figure 5. Simulation of the hydrogenase pulsed ELDOR spectrum for different arrangements of spin projection factors as indicated in Table 1 (solid line Ni-A, dotted line Ni-B).

Table 1. Permutations of Spin Projection Factors K_i (2.28, −0.28, −1.00) with Respect to the Fe Ions of the $[3Fe-4S]^+$ Cluster as Used for Simulation[a]

	Fe1	Fe2	Fe3
A		*b*	
B	2.28	−0.28	−1.00
C	2.28	−1.00	−0.28
D	−1.00	−0.28	2.28
E	−0.28	−1.00	2.28
F	−1.00	2.28	−0.28
G	−0.28	2.28	−1.00

[a] For numbering of the Fe ions, see Figure 1. [b] Spin $S = {}^1/_2$ at an average Fe_i distance of 2.14 nm.

As described in section 2, it is necessary to consider the inner structure of the $[3Fe-4S]^+$ cluster explicitly using the spin projection factors K_i and the distances of the individual Fe ions to the [NiFe] center.

Since the positions of the ions in the $[3Fe-4S]^+$ cluster and the [NiFe] center in the hydrogenase *D. vulgaris* Miyazaki F are known from X-ray analysis, simulations of the pulsed ELDOR spectrum can be employed to assign the spin projection factors to the individual Fe ions by computing spectra for all possible permutations of the three spin projection factors (Table 1). In Figure 5, simulations of an experimental spectrum (Figure 3) for all possible arrangements of spin projection factors are shown. In simulations 5B and 5C, the largest spin projection factor ($K = 2.28$) is located on the Fe ion most remote from the [NiFe] center (Fe1); in simulations 5D and 5E, it is located on the intermediate Fe ion (Fe3). These four simulations bear no resemblance with the experimental spectrum.

Simulation 5F and 5G, where the largest spin projection factor is located on the Fe ion closest to the [NiFe] center, reproduce the main features of the spectrum. Therefore, it is concluded that the largest spin projection factor $K = 2.28$ is associated with the Fe ion closest to the [NiFe] center (Fe2). The differences between simulations 5F and 5G are too small for an unambiguous assignment of the other two spin projection factors to the remaining Fe ions Fe1 and Fe3. It was also possible to simulate the other recorded spectra with this arrangement of spin projection factors.

For the discussion of which effects could affect the reliability of the assignment made above, we first consider the assumed

distance between the spin centers that has been derived from the crystal structure. Minor changes in the distance of the two spin centers could be a consequence of the different sample conditions used in X-ray crystallography and here. As stated above, translating the observed ELDOR frequency into a distance between the spin centers results in an apparent distance of 18 Å. The assignments of the spin projection factors for simulations B−E (in Table 1 and Figure 5) yield peak ELDOR frequencies equal or smaller than the point-dipole approximation (simulation A). Therefore, a distance reduction of at least 3 Å would be necessary for one of the assignments B−E being compatible with the experimental results. We regard alterations in the protein structure of this hydrogenase resulting in a change of 3 Å for a distance of 21 Å to be extremely unlikely.

Another important parameter which strongly affects the calculated frequency spectra is the angle between the g_3-axis of the [NiFe] *g*-tensor and the vector connecting the two spin centers. EPR experiments on single crystals[10] and orientation selected ENDOR experiments on frozen solution[35] have shown virtually identical orientations of the g_3-axis of the [NiFe] *g*-tensor with respect to the protein. According to the protein structure, this yields an angle between the g_3-axis and the vector connecting the spin centers of almost 90°. Any deviation from this almost perpendicular arrangement of these axes would result in a decrease of the calculated dipolar frequencies and, thus, further exclude assignments other than for simulations F and G made above.

Because of the small *g*-anisotropy of the $[3Fe-4S]^+$ cluster, the orientation of this *g*-tensor has little influence on the calculated dipolar spectra, and therefore, potential errors in the orientation do not affect the assignment made above.

5. Conclusions

In this study, the dipolar interaction of two metal centers, the [NiFe] center and the $[3Fe-4S]^+$ cluster in a hydrogenase, was investigated by pulsed ELDOR spectroscopy. The dipolar interaction obtained here was analyzed with respect to distances derived from the X-ray structure and spin projection factors obtained by Mössbauer spectroscopy and showed to be in good agreement with those data.

It was shown that the delocalization of the magnetic moment of the $[3Fe-4S]^+$ cluster over the Fe ions requires a treatment, where the contribution of each individual spin to the total spin is considered explicitly by their spin projection factors. The frequency of the dipolar interaction observed in ELDOR frequencies crucially depends on the arrangement of the spin projection factors within the cluster. By simulating experimental spectra, it is possible to assign spin projection factors of a metal cluster to the ions. For the $[3Fe-4S]^+$ cluster in hydrogenase, it was found that the largest spin projection factor is located on the Fe ion closest to the [NiFe] center. Because of the location of the second spin, the [NiFe] center, the assignment for two of the spin projection factors remains ambiguous. To distinguish between the remaining two possibilities, a second spin would ideally be located in the extension of the Fe1−Fe3 connecting axis. Pulsed ELDOR experiments between the $[3Fe-4S]^+$ cluster and that spin would yield different results, depending on the arrangement of spin projection factors, thus mapping the spin coupling of the $[3Fe-4S]^+$ cluster.

The dependence of the dipolar interaction between a multimeric metal cluster and a second observer spin on the inner structure of the metal cluster has to be considered also in other systems, for example, the tetrameric Mn cluster in photosystem II. We, therefore, conclude that distance determinations between the Mn_4 cluster and other paramagnetic states in photosystem II should be reconsidered.

Acknowledgment. We thank W. Lubitz (TU Berlin) for his continuous support. The *D. vulgaris* Miyazaki F hydrogenase samples were kindly provided by Y. Higuchi (Kyoto, Tokyo). This work has been supported by the Deutsche Forschungsgemeinschaft (SPP 1051, SFB 498 projects C2, C5).

JA027348+

(35) Carepo, M.; Tierney, D. L.; Brondino, C. D.; Yang, T. C.; Pamplona, A.; Telser, J.; Moura, I.; Moura, J. J. G.; Hoffman, B. M. *J. Am. Chem. Soc.* **2002**, *124*, 281−286.